RADIOCHEMISTRY AND RADIOPHARMACEUTICALS

Biodistribution and Dosimetry of N-Isopropyl-*p*-[^{123}I]Iodoamphetamine in the Primate

B. Leonard Holman, Robert E. Zimmerman, Jeffrey R. Schapiro, Michael L. Kaplan, Alun G. Jones, and Thomas C. Hill

Harvard Medical School, Boston, Massachusetts

The biodistribution of N-isopropyl-*p*-[^{123}I]iodoamphetamine (I-123 IMP) in the *Macaca fascicularis* monkey was determined at 15 min and at 1, 4, 24, and 48 hr after intravenous injection. Brain uptake was 7.8% of the injected dose at 1 hr, with little change in concentration between 15 min and 1 hr, falling thereafter. Eye uptake reached a maximum of 0.23% of injected dose at 24 hr, with activity primarily in the pigmented layers. The human absorbed radiation dose was calculated on the basis of biodistribution data. The critical organ is the eye (0.407 rad/mCi of I-123 IMP). The eye dose increased to 1.11 rad/mCi with 4% contamination from I-124 IMP and to 0.535 rad/mCi with 0.4% contamination from I-125 IMP. The absorbed dose to the liver was 0.127 rad/mCi for pure I-123 IMP and the thyroid dose was 0.120 rad/mCi, both increasing with either I-124 or I-125 contamination. While delayed eye uptake has not yet been reported in the human, care should be exercised in limiting the amount of contaminating I-124 or I-125 to the lowest practical level.

J Nucl Med 24: 922–931, 1983

N-isopropyl-*p*-[^{123}I]iodoamphetamine (I-123 IMP) has a number of attributes that make it an attractive choice for cerebral perfusion imaging. It is lipophilic, and after i.v. injection it passes efficiently into the cerebral parenchyma (*1*). Once there, it is either bound to nonspecific receptor sites or is converted to a nonlipophilic metabolite (*2*). Washout from the brain is slow, permitting substantial time for static imaging of cerebral perfusion (*3,4*). Its initial distribution is proportional to cerebral blood flow over a wide range of flows (*5*). The percent injected dose reaching the brain is between 7% and 8% in man, enough to permit high-resolution tomographic or planar imaging (*4*). Initial trials in patients with cerebral vascular disease and epilepsy have been encouraging (*3,6–8*).

The success of I-123 IMP as a measure of cerebral perfusion will depend on its kinetics in the human system. The biodistribution of this tracer will determine the length of time after injection that it reflects cerebral blood flow, the dose of the radiotracer that can be safely administered to patients, and the effect of uptake and metabolism in other organs on the accuracy of cerebral blood-flow measurements. In an effort to determine accurately and quantitatively the biodistribution and dosimetry of I-123 IMP in the highest-order animal in which dissection and in vitro assay is possible, we studied its biodistribution in the monkey *Macaca fascicularis*.

Received Feb. 17, 1983, revision accepted April 11, 1983.

For reprints contact: B. Leonard Holman, MD, Dept. of Radiology, Harvard Medical School, 25 Shattuck St., Boston, MA 02115.

METHODS

Twelve healthy *M. fascicularis* monkeys, six of each sex and 1–3 yr of age, were obtained commercially.* The day after arrival, a fecal flotation analysis for internal parasites gave negative results. After the 9-day quarantine period, each animal was fasted overnight and sedated with 25 mg/kg intraperitoneal pentobarbital sodium, and baseline heart and respiratory rates, rectal body temperatures, and body weights were obtained. The range of body weights was 1.50–1.87 kg for females and

1.60–1.88 kg for males. Blood samples were drawn at this time for hematology and blood chemistry. One monkey was eliminated from the study because of leukopenia and eosinophilia. The remaining 11 animals used in the study all had normal baseline hematology, blood chemistry, and urinalysis values. The I-123 IMP was obtained commercially, with a specific activity of 14.3 mCi/mg (0.07 mg I-123 IMP/mCi). Its radiochemical purity was determined using silica gel-60 plates with methanol/chloroform/glacial acetic acid (15:85:1, v/v/v) as eluent. The amount of free iodine was less than 1% of the radioactive iodine. The proportion of iodine-124 present was determined in a multi-channel analyzer with a Ge(Li) detector and was estimated at 5.22% at the time of injection.

Before tracer injection, the monkeys were anesthetized with pentobarbital sodium (25 mg/kg intraperitoneally). Each animal was given a dose of I-123 IMP such that the mass ratio (weight of test substance/weight of animal) corresponded to the human dosage level currently used in clinical studies: 1.5 mg of N-isopropyl-*p*-iodoamphetamine per 70 kg (0.02 mg/kg).

Two of the monkeys (a male and a female) were anesthetized and killed by intracardiac overdose of sodium pentobarbital at each of the following times after IMP administration: 15 min, and 1, 4, 24, and 48 hr. One male monkey was killed at 5 days after I-123 IMP.

The male monkeys killed at 1 and 24 hr after injection were imaged within 30 min of death, using a large-field-of-view Anger camera with medium energy collimator. A 20% energy window was set symmetrically over the 159-keV photopeak of I-123. One million counts were acquired in the anterior and left lateral projections at 1 hr, and 100,000 counts in each projection at 24 hr. Images were recorded in analog mode on Polaroid film.

At necropsy, all major organs and tissues were removed, blotted, and weighed, with samples placed in tared counting tubes. At the time of death, samples of feces, blood, bile, and urine were placed in tared counting tubes and their weights were determined. Each sample was covered to a height of 3 cm with fluids: Bouin's solution for the testes and 10% neutral buffered formalin for the others.

Both eyes were removed from each monkey and weighed. One was placed in Zenker's solution for 48 hr, then switched into 10% formalin. The vitreous humor was aspirated from the other eye with a 20-gauge needle, placed in another tube, and covered with Zenker's solution. The rest of the eye was placed in a counting tube and covered with Zenker's solution. After samples from the female monkey killed 24 hr after injection were counted, the eye was dissected into lens, retina, cornea, sclera, and optic nerve. The sample called "retina" included retina, pigmented epithelium, and choroid, with ~50% of the total thickness being retina.

The radioactivity in the samples was assayed in a gamma well counter. Two energy windows were used: channel A was set for 100–200 keV to cover I-123, and channel B for 550–850 keV to cover I-124. A series of standards was also counted with each set of samples. The stability of the counting system was checked against cesium-137 during each count sequence.

For each sample and standard, the counts from both channels were corrected for background activity, and the counts in channel A were corrected to remove cross-over from iodine-124. Counts in both channels were then corrected for radioactive decay. Based on these final figures and the weights obtained at necropsy, the biodistribution of I-123 IMP was determined both in terms of the percent injected per dose gram of tissue and percent injected dose per organ/tissue.

Calculations were performed separately for the iodine-123 and iodine-124 counting data. The resulting biodistributions did not differ significantly. Since the channel B measurements required no correction for crossover and gave better counting statistics for the animals killed at the later time points, the values derived from the iodine-124 data were used for dosimetry calculations. It was noted that distribution was independent of sex. Therefore, the biodistribution values used for dosimetry calculations were obtained, when possible, by averaging the data from both animals sacrificed at a given time point.

Absorbed radiation doses to major body organs were determined according to the MIRD (Medical Internal Radiation Dose) Committee's schema for dosimetry calculations (*9–15*). Dose calculations for the eye and its substructures were performed separately using mathematical models of the eye (see Appendix) together with polynomial approximation of the energy absorption parameters of "scaled absorbed-dose" introduced by Berger (*16,17*).

RESULTS

The biodistribution of I-123 IMP in the *M. fascicularis* monkey is presented in Table 1. The brain uptake is prompt, with 5.3% of the injected dose reaching the brain by 15 min and peak uptake (7.8%) at 1 hr. (Data are presented in the text as average values obtained from the male and female monkey at each time point, since there was no significant sex difference.) There is a slight fall in brain activity to 6.3% of the injected dose at 4 hr. Most of the tracer has left the brain by 2 days. The ratio of concentrations between gray and white matter was 2.4 at 15 min, similar at 1 hr (2.2), then fell to 1.8 at 4 hr, 0.6 at 1 day, and 0.5 at 2 days. In other words, the higher concentration in the gray matter was essentially unchanged between 15 min and 1 hr, but had reversed by Day 1, leaving higher concentrations in the white matter than in gray.

TABLE 1. BIODISTRIBUTION OF IODINE-123

	15 min		1 hr		4 hr		24 hr		48 hr		5 days
Sex	M	F	M	F	M	F	M	F	M	F	M
Liver	0.167	0.358	0.346	0.317	0.316	0.247	0.045	0.022	0.005	0.008	0.003
	7.984	15.907	15.898	22.521	14.096	15.693	1.938	1.299	0.335	0.420	0.166
Right kidney	0.213	0.350	0.183	0.253	0.141	0.089	0.019	0.019	0.004	0.005	0.002
	1.320	1.910	0.881	1.141	0.606	0.457	0.106	0.100	0.017	0.021	0.009
Left kidney	0.217	0.377	0.184	0.229	0.150	0.090	0.020	0.017	0.003	0.005	0.002
	1.327	2.023	0.946	1.169	0.669	0.526	0.115	0.097	0.015	0.020	0.009
Spleen	0.123	0.520	0.203	0.201	0.129	0.123	0.021	0.011	0.003	0.003	0.002
	1.200	1.852	1.000	1.072	0.316	0.466	0.139	0.043	0.016	0.009	0.012
Pancreas	0.256	0.598	0.199	0.238	0.188	0.114	0.013	0.009	0.002	0.004	0.001
	0.777	1.712	0.595	0.721	0.732	0.404	0.031	0.031	0.004	0.007	0.003
Rib	0.026	0.037	0.050	0.046	0.025	0.012	0.014	0.003	—	0.000	0.000
Tibia	0.006	0.006	0.004	0.004	0.003	0.033	0.002	0.001	—	0.000	0.000
Marrow	0.027	0.027	0.017	0.025	0.016	0.403	0.004	0.003	—	0.001	0.000
Uterus or	+	0.113	0.052	0.082	0.107	0.044	0.011	0.008	0.001	0.002	0.000
prostate	+	0.048	0.026	0.041	0.009	0.016	0.005	0.004	0.000	0.002	0.000
Right and left	0.025	0.092	0.043	0.086	0.047	0.041	0.011	0.008	0.001	0.002	0.000
gonads	0.048	0.026	0.060	0.033	0.071	0.011	0.012	0.003	0.001	0.001	0.001
Salivary glands	0.146	0.276	0.209	0.225	0.159	0.104	0.013	0.009	0.002	0.003	0.001
(2)	0.096	0.450	0.295	0.569	0.283	0.162	0.019	0.015	0.003	0.005	0.002
Right lachrymal	0.043	0.084	0.107	0.058	0.043	0.041	0.014	0.007	—	0.002	—
gland	0.005	0.013	0.018	0.005	0.009	0.013	0.002	0.001	—	0.000	—
Left lachrymal	0.033	0.086	0.103	0.056	0.061	0.029	0.014	0.008	—	0.002	—
gland	0.009	0.026	0.019	0.005	0.010	0.004	0.002	0.002	—	0.000	—
Stomach	0.047	0.060	0.071	0.068	0.127	0.049	0.011	0.011	0.001	0.004	0.000
	0.599	0.643	0.683	0.895	1.750	0.789	0.135	0.127	0.007	0.072	0.005
Small intestine	0.048	0.094	0.127	0.131	0.129	0.077	0.011	0.010	0.001	0.004	0.001
	2.688	3.196	7.328	9.341	6.708	3.980	0.619	0.584	0.072	0.181	0.061
Large intestine	0.039	0.107	0.100	0.105	0.057	0.044	0.011	0.009	0.001	0.009	0.000
	1.410	3.091	2.807	8.520	4.963	2.107	0.322	0.472	0.089	0.371	0.021
Cecum	0.054	0.110	0.072	0.120	0.086	0.042	0.011	0.008	0.001	0.004	0.001
	1.313	1.433	1.188	4.209	1.847	0.643	0.210	0.301	0.019	0.076	0.011
Feces	0.004	0.033	0.033	0.082	0.015	0.013	0.013	0.011	0.003	0.015	—
Bladder	0.022*	0.043	0.075	0.076	0.215	0.295	0.019	0.018	0.003	0.005	0.001
	0.048	0.067	0.113	0.116	0.368	0.450	0.029	0.025	0.005	0.005	0.002
Urine	0.036	0.047	0.454	0.465	1.056	+	0.027	0.165	0.042	+	0.001
Smooth muscle	0.056	0.039	0.042	0.035	0.025	0.018	0.006	+	0.000	0.001	0.000

(continued)

The concentration in the lung averaged 11.2% of the injected dose at 15 min, with slow washout after that time. Tracer concentration was highest at 15 min in most organs—including the kidneys, spleen, pancreas, adrenal glands, and heart—then fell gradually for the first 24 hr after injection, approaching background levels by 48 hr. Uptake in the liver, however, was greatest at 1 hr, with persistently high concentrations at 4 hr and rapid clearance by 1 day.

Uptake of the tracer by the thyroid gland increased steadily until 24 hr after injection (to 0.2% of dose), and remained at this level for at least 5 days. Concentration in other organs affected by iodine traps was similar, but with more rapid clearance. Tracer concentration peaked in the salivary gland at 1 hr, in the stomach at 4 hr, and in the large intestine between 1 hr and 4 hr.

In the eye the concentration of the tracer steadily increased until reaching maximum activity at 24 hr after injection (0.2% of dose), falling slowly thereafter. Sixty-five percent of the activity was in the tissue specimen containing the retina, choroid, and epithelial pigment; 20% was in the optic nerve; and 15% in the sclera. Uptakes in the cornea and lens were not significantly above background.

In the images obtained at 1 hr after injection, activity was concentrated primarily in the brain, lung, and liver (Fig. 1). By 24 hr, activity was most intense in the eye and thyroid gland, with more uniform distribution throughout the remainder of the body than at 1 hr.

The absorbed doses in rad/mCi of injected iodine-123 IMP (with contamination levels of I-124 ranging from 0 to 10%) are given in Table 2. A similar table for con-

TABLE 1. *(continued)*

	15 min		1 hr		4 hr		24 hr		48 hr		5 days
Sex	M	F	M	F	M	F	M	F	M	F	M
Skeletal muscle	0.073	0.019	0.046	0.009	0.022	0.026	0.004	0.003	0.000	0.001	0.000
Fat	0.019	0.064	0.026	0.028	0.089	0.025	0.004	0.003	0.001	0.002	0.000
Skin	0.014	0.054	0.039	0.048	0.032	0.041	0.058	0.044	0.026	0.023	0.020
Brain	0.078	0.107	0.167	0.119	0.122	0.119	0.024	0.018	0.002	0.003	0.002
	5.116	5.404	9.262	6.311	6.613	6.067	1.612	0.881	0.112	0.145	0.072
Gray matter	0.109	0.134	0.167	0.160	0.158	0.144	0.025	0.013	0.002	0.003	0.002
White matter	0.045	0.064	0.080	0.071	0.085	0.083	0.032	0.029	0.004	0.006	0.002
Sciatic nerve	0.032	0.042	0.023	0.024	0.044	0.217	0.039	0.032	0.006	0.012	0.000
Cerebellum	0.086	0.128	0.127	0.135	0.118	0.094	0.018	0.011	0.002	0.003	0.001
	0.511	0.593	0.620	0.541	0.603	0.332	0.063	0.043	0.008	0.011	0.006
Brain stem	0.081	0.113	0.131	0.131	0.132	0.108	0.023	0.021	0.002	0.003	0.002
	0.294	0.137	0.279	0.233	0.256	0.228	0.078	0.032	0.005	0.004	0.004
Corpus callosum	0.080	0.056	0.090	0.083	0.091	0.100	0.023	0.014	0.002	0.004	0.001
	0.063	0.033	0.063	0.021	0.093	0.041	0.011	0.007	0.001	0.002	0.001
Gall bladder	0.109	0.164	0.175	0.164	0.509	0.210	0.042	0.037	0.004	0.020	0.002
	0.176	0.063	0.461	0.049	0.295	0.105	0.051	0.057	0.003	0.019	0.000
Injection site	+	+	+	+	0.041	+	+	+	+	0.017	+
Mesenteric lymph node	0.037	0.145	0.106	0.155	0.078	0.093	0.016	0.004	0.002	0.000	—
Cervical lymph node	0.055	0.128	0.100	0.133	0.084	0.105	0.014	0.009	—	0.002	—
Right eye vitreous humor	0.001	0.001	0.003	0.002	0.002	0.001	0.001	0.001	—	0.000	—
Rest of right eye	0.070	0.105	0.074	0.082	0.193	0.191	0.234	0.219	0.079	0.062	0.145
Adrenal glands	0.315	0.526	0.226	0.237	0.292	0.216	0.025	0.017	0.005	0.004	0.001
(2)	0.089	0.139	0.093	0.091	0.120	0.108	0.013	0.008	0.003	0.002	0.000
Thyroid gland	0.122	0.223	0.198	0.123	0.181	0.329	1.477	0.657	0.844	1.268	0.645
	0.036	0.045	0.048	0.025	0.044	0.123	0.243	0.200	0.216	0.254	0.227
Pituitary gland	0.218	0.219	+	0.309	0.272	0.095	0.005	—	—	—	—
Blood	0.016	0.032	0.022	0.036	0.017	0.028	0.011	0.011	0.003	0.002	0.000
Heart	0.109	0.256	0.096	0.094	0.069	0.043	0.013	0.007	0.001	0.002	0.000
	1.032	2.207	0.725	0.777	0.594	0.350	0.092	0.042	0.005	0.013	0.003
Lungs	0.805	0.541	0.485	0.640	0.614	0.309	0.044	0.027	0.015	0.016	0.044
	10.880	11.483	9.212	8.417	6.420	3.369	1.104	0.278	0.264	0.156	0.081

$\frac{\text{\% Injected dose per gram}}{\text{\% Injected dose per organ}}$

+ = No sample taken.
— = Calculated value <0.
* Bladder with prostate.

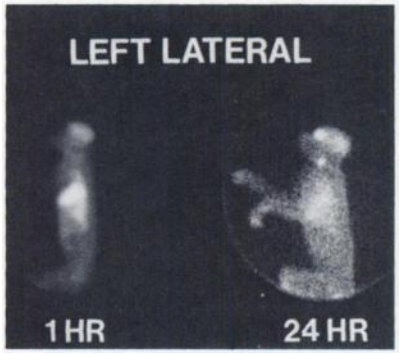

FIG. 1. Lateral scintiphotos made 1 hr (left) and 24 hr (right) after injection of I-123 IMP. Brain, lung, and liver uptakes are high at 1 hr, whereas eye and thyroid have highest concentrations of I-123 IMP at 24 hr.

tamination levels of I-125 IMP ranging from 0 to 1% is presented in Table 3. For pure I-123 IMP, the total-body dose is 0.024 rad/mCi. Aside from the eye dose, the organs with the highest radiation doses are the liver (0.127 rad/mCi), the thyroid (0.120 rad/mCi), and the upper large intestine (0.101 rad/mCi). The dose to the brain is 0.060 rad/mCi, and to the eye 0.407 rad/mCi. Assuming that the activity in the tissue sample containing retina, pigmented epithelium, and choroid is concentrated entirely in the retina (the worst case), the dose to the retina is 8.16 rad/mCi. If the tracer were concentrated in the choroid, the dose to the retina would be 1.62 rad/mCi. With tracer concentrated in the pigmented epithelium, the dose to the retina would be 4.66 rad/mCi. With the activity uniformly distributed throughout

TABLE 2. DOSE (rad) PER mCi INJECTED I-123 IMP, WITH I-124 IMP (%) CONTAMINATION (see Appendix)

Target organ	0%	1%	2%	3%	4%	5%	6%	7%	8%	9%	10%
Adrenals	0.078	0.086	0.094	0.101	0.109	0.117	0.125	0.133	0.140	0.148	0.156
Bladder wall	0.072	0.079	0.087	0.094	0.102	0.109	0.117	0.124	0.132	0.139	0.147
Bone	0.018	0.019	0.021	0.022	0.024	0.025	0.027	0.028	0.030	0.031	0.033
Stomach wall	0.042	0.046	0.050	0.054	0.058	0.061	0.065	0.069	0.073	0.077	0.081
Small intestines	0.092	0.101	0.109	0.118	0.127	0.135	0.144	0.153	0.161	0.170	0.179
Upper large intestine wall	0.101	0.110	0.120	0.129	0.138	0.148	0.157	0.166	0.175	0.185	0.194
Lower large intestine wall	0.082	0.090	0.098	0.107	0.115	0.123	0.131	0.140	0.148	0.156	0.164
Kidneys	0.067	0.073	0.080	0.086	0.093	0.099	0.105	0.112	0.118	0.125	0.131
Liver	0.127	0.139	0.150	0.162	0.173	0.185	0.196	0.208	0.219	0.231	0.242
Lungs	0.064	0.070	0.076	0.083	0.089	0.095	0.101	0.108	0.114	0.120	0.126
Marrow	0.029	0.031	0.033	0.035	0.038	0.040	0.042	0.044	0.046	0.048	0.050
Muscle	0.020	0.022	0.024	0.026	0.028	0.030	0.032	0.034	0.036	0.038	0.040
Ovaries	0.045	0.049	0.053	0.057	0.061	0.065	0.069	0.073	0.076	0.080	0.084
Pancreas	0.073	0.079	0.085	0.092	0.098	0.104	0.110	0.117	0.123	0.129	0.135
Skin	0.022	0.028	0.033	0.039	0.044	0.050	0.055	0.061	0.066	0.072	0.077
Spleen	0.055	0.060	0.066	0.071	0.076	0.082	0.087	0.092	0.098	0.103	0.108
Testes	0.024	0.027	0.029	0.032	0.035	0.037	0.040	0.043	0.045	0.048	0.051
Thyroid	0.120	0.202	0.285	0.367	0.450	0.532	0.615	0.697	0.780	0.862	0.944
Uterus	0.029	0.031	0.034	0.036	0.039	0.041	0.043	0.046	0.048	0.050	0.053
Brain	0.060	0.066	0.072	0.078	0.084	0.090	0.096	0.102	0.108	0.114	0.120
Retina (retinal source)	8.16	8.97	9.78	10.58	11.39	12.20	13.01	13.82	14.62	15.43	16.24
Retina (pig. ep. source)	4.66	5.25	5.84	6.43	7.02	7.62	8.21	8.80	9.39	9.98	10.57
Retina (choroid source)	1.62	2.07	2.52	2.98	3.43	3.88	4.33	4.78	5.24	5.69	6.14
Retina (uniform source)	4.61	5.23	5.84	6.46	7.07	7.69	8.30	8.92	9.53	10.15	10.76
Lens	0.428	0.700	0.972	1.244	1.516	1.788	2.060	2.332	2.604	2.876	3.148
Eye	0.407	0.583	0.759	0.935	1.111	1.287	1.463	1.639	1.815	1.991	2.167
Total body	0.024	0.026	0.029	0.031	0.034	0.036	0.038	0.041	0.043	0.045	0.048

the three layers in the tissue sample, the dose would be 4.61 rad/mCi.

The absorbed dose to the lens from pure I-123 is quite small (0.428 rad/mCi), even though we assumed uptake in the pigmented layer of the iris, which is in direct contact with the lens.

Because the eye and thyroid are relatively small organs and contain high concentrations of the radiotracer, they are greatly affected by contamination with either I-124 or I-125 IMP. In the case of the eye, the dose increases from 0.407 rad/mCi with no I-124 IMP to 1.11 rad/mCi with 4% contamination. For the thyroid, the increase in dose is from 0.120 to 0.450 rad/mCi. For I-125 IMP contamination, the radiation dose to the eye rises from 0.407 with 0% contamination to 0.535 rad/mCi with 0.4% I-125 IMP. For the thyroid, the increase is from 0.120 to 0.176 rad/mCi with 0% to 0.4% I-125. It is in the lens that the difference in absorbed dose between I-124 and I-125 is greatest, because of the effect of nonpenetrating radiation from the iris. The absorbed dose to the lens is 1.52 rad/mCi for I-123 IMP with 4.0% I-124, and 0.496 rad/mCi for I-123 IMP with 0.4% I-125. The radiation doses to the larger organs and to the total body are affected to only a small extent by I-124 and I-125 contamination at the levels encountered in commercial I-123 preparations.

DISCUSSION

Permeability of the blood-brain barrier is limited to a small family of compounds made up almost exclusively of carbon, oxygen, and nitrogen. As a result, we have seen pioneering efforts in the fields of neurophysiology and neurochemistry using positron-emitting isotopes of these elements and the light halogen, fluorine. At present, positron-emission computerized tomography (PET) is limited to a few centers because it needs costly on-site cyclotrons and on-site production facilities for radiochemical and radiopharmaceutical synthesis. If the impressive results that have been obtained with PET are to have any widespread application in clinical practice, radioagents and instrumentation must be available commercially and be sufficiently inexpensive so that all nuclear medicine facilities can perform these functional cerebral studies.

Recently a family of amines that meets the two requirements for brain imaging—blood-brain barrier

TABLE 3. DOSE (rad) PER MCI INJECTED I-123 IMP FOR % CONTAMINATION I-125

Target Organ	0.0%	0.1%	0.2%	0.3%	0.4%	0.5%	0.6%	0.7%	0.8%	0.9%	1.0%
Adrenals	0.078	0.078	0.078	0.078	0.078	0.078	0.078	0.079	0.079	0.079	0.079
Bladder wall	0.072	0.072	0.072	0.072	0.072	0.072	0.072	0.073	0.073	0.073	0.073
Bone	0.018	0.018	0.018	0.018	0.018	0.018	0.018	0.018	0.018	0.018	0.018
Stomach wall	0.042	0.042	0.042	0.042	0.042	0.042	0.042	0.042	0.042	0.042	0.042
Small intestines	0.092	0.092	0.092	0.092	0.092	0.092	0.093	0.093	0.093	0.093	0.093
Upper large intestine wall	0.101	0.101	0.101	0.101	0.101	0.102	0.102	0.102	0.102	0.102	0.102
Lower large intestine wall	0.082	0.082	0.082	0.082	0.082	0.082	0.083	0.083	0.083	0.083	0.083
Kidneys	0.067	0.067	0.067	0.067	0.067	0.067	0.067	0.068	0.068	0.068	0.068
Liver	0.127	0.127	0.127	0.127	0.128	0.128	0.128	0.128	0.128	0.128	0.128
Lungs	0.064	0.064	0.064	0.064	0.064	0.064	0.064	0.065	0.065	0.065	0.065
Marrow	0.029	0.029	0.029	0.029	0.029	0.029	0.029	0.029	0.029	0.029	0.029
Muscle	0.020	0.020	0.020	0.020	0.020	0.020	0.020	0.020	0.020	0.020	0.020
Ovaries	0.045	0.045	0.045	0.045	0.045	0.045	0.045	0.045	0.045	0.045	0.045
Pancreas	0.073	0.073	0.073	0.073	0.073	0.073	0.073	0.073	0.074	0.074	0.074
Skin	0.022	0.022	0.022	0.022	0.022	0.023	0.023	0.023	0.023	0.023	0.023
Spleen	0.055	0.055	0.055	0.055	0.056	0.056	0.056	0.056	0.056	0.056	0.057
Testes	0.024	0.024	0.024	0.024	0.024	0.024	0.024	0.024	0.024	0.024	0.024
Thyroid	0.120	0.134	0.148	0.162	0.176	0.190	0.204	0.218	0.232	0.247	0.261
Uterus	0.029	0.029	0.029	0.029	0.029	0.029	0.029	0.029	0.029	0.029	0.029
Brain	0.060	0.060	0.060	0.060	0.060	0.060	0.060	0.060	0.060	0.060	0.060
Retina (retinal source)	8.16	9.09	10.02	10.95	11.88	12.81	13.74	14.67	15.60	16.53	17.46
Retina (pig. ep. source)	4.66	4.80	4.93	5.07	5.20	5.34	5.47	5.61	5.74	5.88	6.01
Retina (chorold source)	1.62	1.63	1.64	1.65	1.66	1.67	1.69	1.70	1.71	1.72	1.73
Retina (uniform source)	4.61	5.04	5.46	5.89	6.32	6.75	7.17	7.60	8.03	8.45	8.88
Lens	0.428	0.445	0.462	0.479	0.496	0.513	0.530	0.547	0.564	0.581	0.598
Eye	0.407	0.439	0.471	0.503	0.535	0.568	0.600	0.632	0.664	0.696	0.728
Total body	0.024	0.024	0.024	0.024	0.024	0.024	0.024	0.024	0.024	0.024	0.024

permeability and retention in the brain parenchyma—have been synthesized and labeled with iodine-123 (*1*,*2*,*18*). One of the most promising of these tracers, I-123 IMP, has already been used in man and is undergoing extensive clinical trials (*4*). We describe here the kinetics of this tracer in the monkey in order to provide a basis for human dosimetry calculations and to determine the effects of those kinetics on brain uptake and retention.

The concentration of I-123 IMP in the monkey brain, 6% to 9% of the injected dose at 1 hr, is comparable to in vivo estimates in man (*4*). The uptake increases a little from 15 min to 1 hr, probably due to continual washout of the tracer from the lungs. The ratio of activity between gray and white matter is constant from 15–60 min in the monkey. Rapin et al. found concentration ratios of 10:1 at 3 min after injection, falling to 4:1 by 1 hr, and suggested the need for early imaging because of redistribution of the tracer (*19*). We find no evidence of redistribution in the brain between 15 min and 1 hr and feel that I-123 IMP reflects relative cerebral perfusion during that time. By 4 hr, however, the ratio for gray matter over white has fallen and the tracer is no longer an accurate measure of cerebral blood flow. The gray-to-white ratio reverses by 24 hr, probably indicating more rapid washout from the gray due to its higher blood flow.

The behavior of I-123 IMP in the liver, with slow accumulation during the first hour after injection, suggests accumulation of metabolites in the liver in addition to an initial accumulation of IMP itself. Other systemic organs show more rapid accumulation, probably of unaltered IMP, with fairly rapid clearance mirroring brain kinetics.

There is substantial and persistent accumulation of the tracer in the thyroid, indicating breakdown of the radiopharmaceutical by 24 hr, with detachment and trapping of iodine. The persistently high concentration in the thyroid indicates the need for blocking the gland with Lugol's solution or potassium perchlorate when nonthyroid imaging is performed in patients. Blocking will have to be continued for some time after injection of the pharmaceutical if significant amounts of I-124 or I-125 are present as contaminants.

The high concentration of iodoamphetamine analogs in the pigmented portion of the eye has been observed in dogs, rodents, and monkeys anesthetized with pentobarbital (*2*,*20*) but not in monkeys anesthetized with ketamine (*2*) nor in man (*3*). In our study, pentobarbital was administered 15 min before tracer injection and

immediately before death. It would be unlikely that the anesthetic would augment eye uptake, particularly in animals killed 2 to 5 days after injection. An alternative hypothesis for the discrepancy in the amount of tracer uptake between monkeys and adult humans is that uptake may be related to melanin production in the pigmented layers of the eye. This process is completed in embryo in humans. We may have seen uptake in our young monkeys, still forming melanin in the pigmented choroid and iris of their eyes, whereas humans, who have completed their eye melanin production, have little or no I-123 IMP uptake. The kinetics of eye uptake suggest accumulation of a metabolite that is released either from the brain or liver, because the concentration in the eye is initially low and reaches maximum values only at 24 hr and 48 hr after injection.

Even at the dose levels calculated from the monkey data, the radiation exposure presents no significant health problem for anticipated 3- 5-mCi dosages in man. Lieberman has shown that no histopathological changes occur in the retina with absorbed radiation doses from I-131 up to 1200 rad (*21*). Functional changes can be detected by electroretinograms only with absorbed doses greater than 600 rad to the retina. The absorbed radiation dose to the retina from I-123 IMP is orders of magnitude less, even if we assume that eye uptake in man will be as high as in our monkeys.

A routine TCT scan, with and without contrast, results in an absorbed radiation dose of 14 rad to 20 rad to the lens (*22*). Thus, while the biological effectiveness of the two types of radiation are not entirely comparable, I-123 IMP results in a radiation dose to the lens several orders of magnitude less than TCT scanning. Since the minimum cataractogenic dose for patients receiving radiation over a 3- to 12-wk interval is 400 rad, both TCT scanning and I-123 IMP brain imaging are safe with regard to dose to the lens (*23*).

There are currently two ways of producing I-123: (a) the indirect method, $^{127}I(p,5n)^{123}Xe \rightarrow {}^{123}I$, which also produces I-124 as an impurity; and (b) the direct method. The latter is more versatile, requiring proton energies of only 24–28 MeV, but the I-124 contaminant results in degradation of spatial resolution because of its high-energy gamma. Currently the bulk of I-123 supplied in the United States is produced by the direct method. The indirect method requires substantially higher proton energies (between 55 MeV and 70 MeV), but the resultant I-123 has better imaging properties since the I-125 emissions are low in energy.

The radiation doses from IMP labeled with I-123 produced by the two methods are surprisingly similar. The contaminants have little effect on the dose to the total body, to large organs, or to organs that receive only a small percentage of the injected dose. The effect of contamination is striking, however, on the thyroid and the eye, since they receive substantial concentrations of the tracer and they are relatively small organs. While the thyroid can be blocked and the eye doses calculated from the monkey data probably overestimate those for the adult human, it would be prudent to use I-123 with as little as possible contamination from either I-124 or I-125. If the direct method is used, I-124 concentrations should be kept to less than 4% by using the tracer within 24 hr of production. While some commercial suppliers of I-123 produced by the indirect method guarantee that I-125 will be no higher than 1.9% of the total iodine activity, contamination levels can be kept at less than 0.4% by current production techniques. Contamination levels of I-125 greater than 0.4% should probably be avoided for brain imaging with I-123 IMP.

FOOTNOTES

* Charles River Research Primates Corporation, Port Washington, New York.

ACKNOWLEDGMENTS

We acknowledge Alice Carmel, Rebecca Taub, and Diane Johnson for their technical assistance, and Medi-Physics, Inc., Emeryville, California, for supplying I-123 IMP.

APPENDIX

For all important sources of I-123 IMP uptake, values of the percent injected dose per organ or tissue were plotted on semilog paper as a function of time. Straight-line segments were used to approximate the various contours of the resulting graphs. These approximations determined an analytical description of the biological time course of the tracer. For each organ or tissue, the time course f(t) was described by a piecewise function composed of single-term exponential segments of the form:

$$F(t) = B \cdot \exp(M \cdot t \cdot \ln 10) \text{ for } TI < t < TF,$$

where B is the intercept, and M is the slope of the underlying linear approximation; TI and TF are the endpoints of the appropriate time interval. Expressions for the activities of I-123, I-124, and I-125 were then obtained by multiplying each time-course function by the decay factor $\exp(-\ln 2 \cdot t/T_{1/2})$. ($T_{1/2}$ is the half-life of the appropriate isotope.) Finally, these activity functions were integrated with respect to time to determine the cumulated activity $\tilde{A}$ for each of the three iodine isotopes in each of the selected organs or tissues.

As the dosimetry calculations were based on the framework developed by the Medical Internal Radiation Dose Committee (MIRD), the values for the cumulated activity were organized to correspond to the source-organ categories described in MIRD publications (*9,10*). The following assumptions were made in determining cumulated activities for the MIRD-designated source organs:

1. In instances where total tissue weight was unknown (i.e., muscle, bone, skin, fat, blood, urine), a value was assigned such that the ratio of tissue weight to total body weight agreed with the corresponding value for man.

2. In order to incorporate the cumulated activity measured in the large intestine and cecum into the MIRD schema, these values were added together and split proportionately by weight between the categories "upper large intestine" and "lower large intestine."

TABLE 4

Radiation categories		Δ_i	Power of polynomial used in approximation
I-123:	500-keV gamma	0.0282	10
	150-keV gamma	0.280	10
	30-keV x ray	0.527	10
	130-keV electron	0.0457	9
	25-keV electron	0.0060	3
	3-keV electron	0.0064	totally nonpenetrating
I-124:	1.5-MeV gamma	0.983	10
	600-MeV gamma	0.810	10
	Annihilation radiation	0.557	10
	30-keV x ray	0.0339	10
	β	0.451	10
	600-keV electron	0.0040	9
	25-keV electron	0.0042	3
	3-keV electron	0.0061	totally nonpenetrating
I-125:	30-keV x ray	0.0901	10
	25-keV electron	0.0196	3
	3-keV electron	0.0221	totally nonpenetrating

3. Red and yellow marrow were grouped together under the category "red marrow."

4. The cumulated activity for the category "total body"—defined as the sum of all cumulated activities not otherwise explicitly assigned to MIRD source organs—was determined by summing the values determined for fat, connective tissue, and blood. Connective tissues were assigned an activity concentration that was the average of the values for muscle and trabecular bone.

All organ weights for man were taken from the Report of the Task Force on Reference Man (*11*). The designation "fat" was assumed to include the Reference Man categories of "subcutaneous fat" and "other separable tissues," whereas the designation "connective tissues" was chosen to encompass the Reference Man categories of "connective tissues" and "cartilage and periarticular tissue."

An average absorbed dose, $\overline{D}$, was calculated for each MIRD-designated target organ according to the standard dose equation:

$$\overline{D} = \sum \tilde{A}_i S_i, \qquad (1)$$

where $\tilde{A}_i$ is the cumulated activity of source organ i, and S_i is the S factor from source organ i to the target organ (*10*). Absorbed doses were determined for an injected dose of 1 mCi of I-123 contaminated by (a) I-124 or (b) I-125.

S factors to the brain and eye have not been published. Dose calculations for these organs required individual consideration of the various radioactive emissions. Since the number of different radiations is large, emission data were organized into several broad categories (*12,13*). Each collection was treated as a single monoenergetic emission with an equilibrium dose constant equal to the sum of the equilibrium dose constants of the component radiations (Table 4).

Using this simplified model of radioactive emission, S factors to the brain were calculated from the defining equation:

$$S = \frac{1}{m} \sum \Delta_i \Phi_i = \sum \Delta_i \Phi_i. \qquad (2)$$

For radiation species i, Δ_i is the equilibrium dose constant (μCi-hr), Φ_i is the absorbed fraction, Φ_i is the specific absorbed fraction (g^{-1}), and m is the mass of the target organ. The average absorbed dose was then determined from Eq. (1). Dose contributions from penetrating radiations were calculated from values of Φ published by Eckerman (*14*). All nonpenetrating radiations originating in the brain were assumed to be internally absorbed. Contributions from both penetrating and nonpenetrating radiations were summed to obtain a total absorbed dose to the brain. As before, absorbed doses were determined for an injected dose of 1 mCi of I-123 contaminated by I-124 or I-125.

Similar calculations were done to estimate the contributions of external source organs to the average absorbed dose to the eye. For all external source organs other than the brain, the assumption was made that specific absorbed fractions to the eye matched those to the brain. For these organs, eye dose contributions were approximated using Eckerman's Φ values for the brain. The specific absorbed fractions to the eye from the brain were derived from Eckerman's values using the reciprocal relation Φ(eye ← brain) = Φ(brain ← eye), which is true for any two organs under the isotropic model commonly adopted in dosimetry calculations (*9*).

Calculation of a self-absorbed dose to the eye required some knowledge of the internal distribution of radioactivity. The counting data from the dissected eye indicated that most of the tracer resided in a three-layer structure composed of the retina, the pigmented epithelium, and the choroid. Based on this information, two eye models were developed in which eye activity was assumed to be concentrated entirely in this three-layer structure. The models were used to calculate specific absorbed fractions from which internal radiation doses could be determined.

The "concentric spherical shell model" treated the eye as a multilayered sphere of radius 1.20 cm. The source structure was modeled as a spherical shell with inner and outer radii of 1.0965 and 1.1250 cm. It consisted of an inner retinal layer of thickness 130 μm, a pigmented epithelial layer of thickness 5 μm, and an outer choroidal layer of thickness 150 μm. Completing the model were a spherical inner volume representing the vitreous humor,

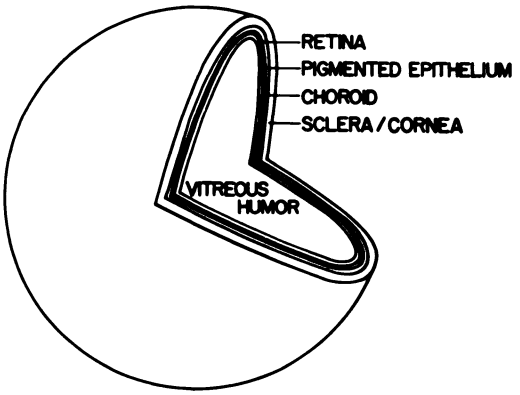

FIG. 2. Spherical-shell model of eye used for dose calculations to retina and eye. (Not drawn to scale.)

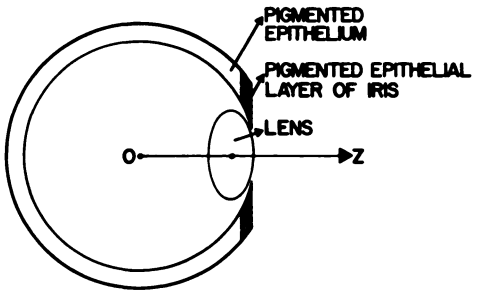

FIG. 3. Longitudinal section of lens model used for calculations of dose to lens. O is origin, z-axis shown. (Not drawn to scale.)

and an outer layer representing the sclera and cornea (Fig. 2) (*15*).

The model was used to calculate internal dose contributions to both the entire eye and the retina. As a specific source layer could not be identified in the three-layer source structure, separate retinal dose calculations were performed for four possible activity distributions: (a) uptake in the retina only, (b) uptake in the pigmented epithelium only, (c) uptake in the choroid only, and (d) uniform uptake in all three layers. The entire eye dose calculation assumed uniform activity distribution throughout the three-layer structure.

The calculation of an absorbed dose to the lens required a more detailed model of the eye and its substructures. Of the three possible source layers, only the pigmented epithelium comes in close proximity to the lens. Therefore, a "lens model" was developed to provide a worst-case approximation to the lens dose by considering an ocular activity distribution concentrated entirely in the pigmented epithelium.

Both the pigmented epithelium and the lens were represented by figures exhibiting radial symmetry around a z-axis drawn through their centers (Fig. 3). The pigmented epithelium was modeled as a section of a spherical shell centered at the origin. The shell had an inner and outer radii of 1.1095 cm and 1.1100 cm. The desired section was obtained by removing a "cap" created by a planar cut perpendicular to the z-axis at a distance of 1.070 cm from the origin. Within this section, the pigmented epithelial layer of the iris was represented by that portion of the shell between the boundary cut and another cut at a distance of 0.934 cm from the origin. The lens was represented by an ellipsoid centered at a distance of 0.890 cm along the z-axis. The hemiaxes of the ellipsoid were 0.467 cm, 0.467 cm, and 0.194 cm (*15*).

Calculations of specific absorbed fraction were based on the general equation:

$$\Phi_i(t \leftarrow s) = \frac{1}{V_s V_t} \iint_{st} \Phi_i(r)\, dV_t\, dV_s, \qquad (3)$$

where s and t refer to the source and target organs, i refers to radiation species and $\Phi(i)$ is the point isotropic specific absorbed fraction at a distance r (*9*).

In order to evaluate this equation for the "concentric spherical shell model," two different spherical coordinate systems were defined. The (ρ,θ,Φ) system had its origin at the center of the model and was used to define a differential source element at P. The (r,θ',Φ') system was centered at P and oriented with the z-axis directed radially Equation (3) was evaluated using the (ρ,θ,Φ) system to integrate over the source region and the (r,θ',Φ') system to integrate over the target region.

$$\Phi_i(t \leftarrow s) = \frac{1}{V_s V_t} \int_{R_i}^{R_o} \int_0^{\pi} \int_0^{2\pi} \int_{r_i(\rho)}^{r_f(\rho)} \int_{\Phi'_i(\rho,r)}^{\Phi'_f(\rho,r)} \int_0^{2\pi} \times \Phi_i(r) r^2 \sin\Phi' \rho^2 \sin\Phi\, d\theta'\, d\Phi'\, dr\, d\theta\, d\Phi\, d\rho$$

$$= \frac{8\pi^2}{V_s V_t} \int_{R_i}^{R_o} \int_{r_i(\rho)}^{r_f(\rho)} \int_{\Phi'_i(\rho,r)}^{\Phi'_f(\rho,r)} \times \Phi_i(r) r^2 \rho^2 \sin\Phi'\, d\Phi'\, dr\, d\rho \qquad (4)$$

(R_i and R_o are the inner and outer radii of the source shell.)

As the target volume approaches zero, Eq. (3) reduces to:

$$\Phi_i(t \leftarrow s) = \frac{1}{V_s} \int_s \Phi_i(r) dV_s \qquad (5)$$

Equation (5) was applied to the "lens model" to determine the dose to the center of the lens due to penetrating radiations. As the deposition of energy by the penetrating radiations is roughly independent of distance for the range of distance involved, this center-of-lens value was assumed to approximate the average absorbed dose to the entire lens. Integration was performed using a spherical coordinate system (r,θ,Φ) having its origin at the center of the lens, and was oriented with the z-axis through the center of the pigmented epithelial shell.

$$\Phi_i(t \leftarrow s) = \frac{1}{V_s} \int_{r_i}^{r_f} \int_{\Phi_i(r)}^{\Phi_f(r)} \int_0^{2\pi} \Phi_i(r) r^2 \sin\Phi\, d\theta\, d\Phi\, dr$$

$$= \frac{2\pi}{V_s} \int_{r_i}^{r_f} \int_{\Phi_i(r)}^{\Phi_f(r)} \Phi_i(r) r^2 \sin\Phi\, d\Phi\, dr \qquad (6)$$

The parameter chosen for integration was Berger's scaled absorbed-dose:

$$F_i(r) = 4\pi\delta r^2 r_{90}\, \Phi_i(r),$$

where δ is the density of the target organ, and r_{90} is the radius of the sphere within which 90% of the energy emitted by the source element is absorbed (*16*). For each of the radiations in the simplified emission model, values of scaled absorbed-dose were obtained from tabulated measurements of radial energy deposition (*16,17*). Polynomial segments were used to approximate these values over distances appropriate to the ranges of the radiations and the dimensions of the eye models. Only the 3-keV electrons were not approximated in this manner, since they were considered to have negligible range.

Substitution of scaled absorbed-dose in Eqs. (4) and (6) gives:

$$\Phi_i(t \leftarrow s) = \frac{2\pi}{\delta V_s V_t r_{90}} \int_{Ri}^{R_o} \int_{r_i(\rho)}^{r_f(\rho)} \int_{\Phi'_i(\rho,r)}^{\Phi'_f(\rho,r)} \times F_i(r) \rho^2 \sin\Phi'\, d\Phi'\, dr\, d\rho \qquad (4a)$$

$$\Phi_i(t \leftarrow s) = \frac{1}{2\delta V_s r_{90}} \int_{r_i}^{r_f} \int_{\Phi_i(r)}^{\Phi_f(r)} F_i(r) \sin\Phi\, d\Phi\, dr \qquad (6a)$$

Using the polynomial approximation, these equations were integrated analytically and the resulting series were evaluated by computer.

The lens dose contribution from nonpenetrating radiations was determined for sources within the pigmented epithelial layer of the iris. Other sources were not considered, since their distance from the lens exceeded the range of the nonpenetrating radiations. Using Eq. (4a), self-absorbed fractions were calculated for the pigmented epithelial layer. Among the fraction of iris radiations that were not reabsorbed, half were assumed to be absorbed by the lens. In this manner, values of Φ (lens ← iris) were determined. The nonpenetrating dose contribution was then calculated from:

$$D = \frac{\text{Vol (iris)}}{\text{Vol (pig ep)}} \tilde{A}_{p.e.} \frac{1}{m_{lens}} \cdot \sum \Delta_i \Phi_i \text{ (lens} \leftarrow \text{iris)}$$

D is dose to the lens from the iris, where Vol is the volume of the iris or pigmented epithelium, and m_{lens} is the mass of the lens.

REFERENCES

1. WINCHELL HS, BALDWIN RM, LIN TH: Development of I-123-labeled amines for brain studies: Localization of I-123 iodophenylalkyl amines in rat brain. *J Nucl Med* 21:940–946, 1980
2. WINCHELL HS, HORST WD, BRAUN L, et al: N-isopropyl-[^{123}I]p-iodoamphetamine: Single-pass brain uptake and washout; binding to brain synaptosomes; and localization in dog and monkey brain. *J Nucl Med* 21:947–952, 1980
3. HILL TC, HOLMAN BL, LOVETT R, et al: Initial experience with SPECT (single-photon computerized tomography) of the brain using N-isopropyl I-123 *p*-iodoamphetamine: Concise communication. *J Nucl Med* 23:191–195, 1982
4. HOLMAN BL, HILL TC, MAGISTRETTI PL: Brain imaging with emission computed tomography and radiolabeled amines. *Invest Radiol* 17:206–215, 1982
5. KUHL DE, BARRIO JR, HUANG SC, et al: Quantifying local cerebral blood flow by N-isopropyl-p-[^{123}I] iodoamphetamine (IMP) tomography. *J Nucl Med* 23:196–203, 1982
6. LEE RGL, HILL TC, HOLMAN BL, et al: N-isopropyl(I-123)p-iodoamphetamine brain scans with single-photon emission tomography: Discordance with transmission computed tomography. *Radiology* 145:795–799, 1982
7. MORETTI J, ASKIENAZY S, RAYNAUD C, LASSEN N, SANABRIA E, SOUSSALINE F, BARDY A, LE PONCIN-LAFITTE M, CARON J-P, CHODKIEWICZ J-P: N-isopropyl-*p*-iodo-amphetamine I-123: an agent for brain imaging with SPECT. In *Radionuclides and the Brain*, Magistretti, PL, Ed. Raven Press, in press
8. MAGISTRETTI P, UREN R, SHOMER D, et al: Emission tomographic scans of cerebral blood flow using I^{123} iodoamphetamine in epilepsy. In *Nuclear Medicine and Biology* II: Raynaud C, Ed. Paris, Pergamon Press, 1982, p 139
9. LOEVINGER R, BERMAN M: A revised schema for calculating the absorbed dose from biologically distributed radionuclides. MIRD Pamphlet No. 1 Revised, New York, Society of Nuclear Medicine, March 1976
10. SNYDER WS, FORD MR, WARNER GG, WATSON SB: *"S" absorbed dose per unit cumulated activity for selected radionuclides and organs. MIRD Pamphlet No. 11.* New York, Society of Nuclear Medicine, Oct 1975
11. SNYDER WS, COOK MS, RASSET ES, et al: Report on the Task Group on Reference Man, ICRP Publication No. 23, Pergamon Press, 1975
12. DILLMAN LT, VON DER LAGE FC: *Radionuclide decay schemes and nuclear parameters for use in radiation dose estimates. MIRD Pamphlet No. 10.* New York, Society of Nuclear Medicine, Sept 1975
13. NASS HW: New I-123 nuclear decay data. *J Nucl Med* 20:1216–1217, 1979
14. ECKERMAN KF, CHRISTY M, WARNER GG: Dosimetric evaluation of brain scanning agents. In *Third International Radiopharmaceutical Dosimetry Symposium.* Watson EA, Schlafke-Stelson AT, Coffey JL, Cloutier RJ, Eds. HHS Publication FDA 81-8166, Bureau of Radiological Health, 1981, pp 527–540
15. *Morris' Human Anatomy—A Complete Systematic Treatise.* Anson BJ, Ed. New York, The Blakiston Division, McGraw-Hill Company, 1966
16. BERGER MJ: *Distribution of absorbed dose around point sources of electrons and beta particles in water and other media, MIRD Pamphlet No. 7.* New York, Society of Nuclear Medicine, March 1971
17. BERGER MJ: Energy disposition in water by photons from point isotropic sources, MIRD Pamphlet No. 2, *J Nucl Med* (Suppl 1):15–25, 1968
18. KUNG HF, TRAMPOSCH KM, BLAU M: A new brain perfusion imaging agent: [I-123]HIPDM:N,N,N′-trimethyl-n′-[2-hydroxy-3-methyl-5-iodobenzyl]-1,3-propanediamine. *J Nucl Med* 24:66–72, 1983
19. RAPIN J-R, LE PONCIN-LAFITTE M, DUTERTE D, ASKIENAZY S, LASSEN N, MORETTI J-L, REYNAUD C, COORNAERT S, BARDY A, DESPLANCES G: Radiopharmacological studies of isopropyl-iodoamphetamine. In *Radionuclides and the Brain.* Magistretti, PL, Ed. Raven Press (in press)
20. SARGENT T III, BRAUN G, BRAUN U, et al: Brain and retina uptake of a radio-iodine labeled psychotomimetic in dog and monkey. *Commun Psychopharm* 2:1–10, 1978
21. LIEBERMAN LM: The effect of radiation on the retina of the dog. PhD Dissertation, Univ. of Michigan, Ann Arbor, 1970
22. RICE JF, BANKS TE: Normal and high accuracy computed tomography of the brain: dose and imaging considerations. *J Comput Assisted Tomogr* 3:497–502, 1979
23. MERRIAM GR JR, FOCHT EF: A clinical study of radiation cataracts and the relationship to dose. *Am J Roentgen* 77: 759–785, 1957